energies

MDPI

Article

Leaching via Weak Spots in Photovoltaic Modules

Jessica Nover [1], Renate Zapf-Gottwick [1,*], Carolin Feifel [2], Michael Koch [2] and Juergen Heinz Werner [1]

[1] Institute for Photovoltaics and Research Center SCoPE, University of Stuttgart, 70569 Stuttgart, Germany; jessica.nover@ipv.uni-stuttgart.de (J.N.); juergen.werner@ipv.uni-stuttgart.de (J.H.W.)
[2] Institute for Sanitary Engineering, Water Quality, and Solid Waste Management, University of Stuttgart, 70569 Stuttgart, Germany; carolin.feifel@iswa.uni-stuttgart.de (C.F.); Michael.Koch@iswa.uni-stuttgart.de (M.K.)
* Correspondence: renate.zapf-gottwick@ipv.uni-stuttgart.de

Abstract: This study identifies unstable and soluble layers in commercial photovoltaic modules during 1.5 year long-term leaching. Our experiments cover modules from all major photovoltaic technologies containing solar cells from crystalline silicon (c-Si), amorphous silicon (a-Si), cadmium telluride (CdTe), and copper indium gallium diselenide (CIGS). These technologies cover more than 99.9% of the world market. We cut out module pieces of 5 × 5 cm^2 in size from these modules and leached them in water-based solutions with pH 4, pH 7, and pH 11, in order to simulate different environmental conditions. Unstable layers open penetration paths for water-based solutions; finally, the leaching results in delamination. In CdTe containing module pieces, the CdTe itself and the back contact are unstable and highly soluble. In CIGS containing module pieces, all of the module layers are more or less soluble. In the case of c-Si module pieces, the cells' aluminum back contact is unstable. Module pieces from a-Si technology also show a soluble back contact. Long-term leaching leads to delamination in all kinds of module pieces; delamination depends strongly on the pH value of the solutions. For low pH-values, the time dependent leaching is well described by an exponential saturation behavior and a leaching time constant. The time constant depends on the pH, as well as on accelerating conditions such as increased temperature and/or agitation. Our long-term experiments clearly demonstrate that it is possible to leach out all, or at least a large amount, of the (toxic) elements from the photovoltaic modules. It is therefore not sufficient to carry out experiments just over 24 h and to conclude on the stability and environmental impact of photovoltaic modules.

Keywords: leaching; long term; photovoltaic modules; delamination; solubility

Citation: Nover, J.; Zapf-Gottwick, R.; Feifel, C.; Koch, M.; Werner, J.H. Leaching via Weak Spots in Photovoltaic Modules. *Energies* **2021**, *14*, 692. https://doi.org/10.3390/en14030692

Academic Editor: Emmanuel Kymakis
Received: 19 November 2020
Accepted: 26 January 2021
Published: 29 January 2021

1. Introduction

Photovoltaic (PV) modules are not a niche product anymore. The market started with an installed capacity of 20 MW in the early 1990s and increased up to 635 GW of total installed PV modules worldwide at the end of 2019 [1]. By assuming an average lifetime of 30 years, we have to deal with an increasing amount of waste from PV modules of up to 1.7 million tonnes until 2030 [2].

In principle, photovoltaics are a green technology; however, some PV modules contain toxic elements such as lead in the solder ribbons and metalization pastes, or even worse, such as in CdTe technology, the toxic elements Cd and Te in the photoactive layer itself. Many modules using copper indium gallium diselenide (CIGS) also contain cadmium in the so-called CdS buffer layer of the CIGS cells. This situation is mainly possible because PV modules are still excluded from the EU Directive on the restriction of hazardous substances (ROHS 2) in electrical and electronic equipment. This exclusion will remain until the next review of the RoHS 2, which is planned for 2021 [3]. For all other electric and electronic equipment (EEE) on the EU market, the tolerated maximum concentrations by weight in homogeneous materials for lead (Pb) and cadmium (Cd) are 0.1% and 0.01%, respectively. Clearly, in the case of the compounds CdS or CdTe, with 50% of the mass being Cd,

the RoHS is not obeyed. However, also the technology of modules with crystalline Si cells has a problem with RoHS, although it could easily be overcome by using cell connectors without lead (usually, the solder contains about 40% lead) in the solder. The tiny amount of Pb in the metallization pastes could be kept below the RoHS limits. In 2019, the amount of lead-free metalization pastes in the case of silicon (Si) solar cells was only 30% [4]. At the same time, the world market share of lead-containing solder for cell connectors was over 90% [4].

Most probably, photovoltaic modules, which contain toxic substances, are safe for the users and the environment, at least as long as the modules are not damaged. Nevertheless, what happens if modules are damaged? What happens at the end of their use? Are they "donated" or "exported" like old cars, other old electronic equipment, and waste to countries outside the EU? In the worst case, finally, wherever it may be, the modules are crushed and/or discarded in landfills. What could happen with the toxic elements? In fact, it is no longer a question if these substances are released into in the environment: several studies proved they do and that the release depends on the pH-value of the leaching solvents, as well as on the redox conditions [5–10]. A literature review can be found in [11].

Despite of all these studies [5–11], several questions are open: How are the toxic substances released? What are the weak spots in the modules? Does leaching only occur in the case of delaminated modules, i.e., in modules, that have lost the front glass? In this case, in particular for thin film modules, it would be understandable that the toxic substances are leached from, for example, the CdTe layers, which are no longer protected by the front glass. Does it work the other way around: Are the thin layers leached from the edges of the module (pieces) leading, finally, to delamination? Clearly, after delamination, the leaching would then be accelerated even more, because the leaching solution is now able to attack the thin layers not only from the edges, but also from the surface. Are there any potentially accelerating parameters, like agitation or temperature, regarding the leaching?

The present contribution gives answers to most of these questions via a long-term study. In contrast to previous work, our leaching tests are not only conducted over 24 h as requested by standard leaching tests [12–15], but for more than 1.5 year; some of our results are even taken after almost two years. Furthermore, we analyze not only eluted amounts of toxic substances like cadmium (Cd) and lead (Pb), but also other elements present in the module layers such as zinc (Zn), tellurium (Te), indium (In), gallium (Ga), selenium (Se), aluminum (Al), molybdenum (Mo), and copper (Cu), to identify soluble and, therefore, weak layers in PV modules. Parts of the experimental details were published earlier in German [16]; some results about the leaching of Cd, Te, and Pb up to day 360 were published earlier by us [10]. We find, that, finally, the modules delaminate because of the leaching from the edges of the module pieces. In all kinds of modules, at least one of the layers of the different cell types represents a weak path for the leaching. In the case of CdTe module pieces, the CdTe layer itself and the Mo contact are soluble. In the case of CIGS module pieces, the Zn front contact, the Mo back contact, and the Cd-containing buffer layer are susceptible to strong leaching. For crystalline silicon module pieces, the Al back contact is a weak spot; for amorphous silicon (a-Si) module pieces, also the back contact (Ni) and the intermediate layer containing Zn are identified as weak spots.

Section 2 of the present contribution describes the sample preparation and the leaching conditions and shows how we determine the total amount of elements within each type of our investigated solar modules. Section 3 presents our leaching results. We measured for more than 1.5 years, not only at room temperature, but also at increased temperature, as well as under accelerated leaching conditions. The leaching time constant depends on the module type, as well as on the leaching conditions. Section 4 identifies the weak spots for each particular module type. Section 5, finally, concludes that the amount of leached out elements after 1.5 years in some cases exceeds the value after one day by more than two orders of magnitude. Thus, leaching experiments, which are just carried out over one day, are valuable. However, statements about the stability and environmental noxiousness of photovoltaic layers are highly questionable when based on such short-term measurements.

2. Materials and Methods

2.1. Sample Preparation and Experimental Conditions

For cutting the module pieces with well-defined sizes and edges, we applied water jet cutting to get samples from the four major commercial PV technologies: crystalline silicon (c-Si), amorphous silicon (a-Si), cadmium telluride (CdTe), and copper indium gallium diselenide (CIGS). The module pieces are cut in a way that all module pieces contained at least one solder ribbon, but no parts of the frame, module boxes, or cables. The sample size of the module pieces for the leaching experiments was 5×5 cm^2.

The leaching experiments were carried out under three different conditions, in order to identify potential accelerating conditions:

- Room temperature $T_{RT} = 25\,^{\circ}$C, no agitation;
- Room temperature $T_{RT} = 25\,^{\circ}$C, with agitation (orbital shaking with rotational speed $n = 100\,\mathrm{min}^{-1}$);
- Increased temperature $T_{IT} = 40\,^{\circ}$C, with agitation (orbital shaking with rotational speed $n = 100\,\mathrm{min}^{-1}$).

For all experiments, we used high-density polyethylene (HDPE) bottles supplied with the leaching solution with a 1000 mL volume and two pieces from the very same module; see also [10]. The samples were not fixed in the bottles, and the bottles were lightproof. From earlier experiments (not presented here), we know that light accelerates leaching. However, light leads also to the production of alga, in particular for the long leaching times we are using. Alga production changes the experimental conditions and makes the leaching experiments less reproducible. Therefore, for the experiments presented here, we decided to use lightproof bottles. In order to increase the significance and validity of our experiments even more, each experiment was conducted in triplicate (this means three bottles, each one filled with two samples) for every condition. The leaching data, i.e., the concentration of a particular element in the solutions, are given as the mean value of the probes taken from the three bottles.

The leaching solutions with three different pHs covered the pH range of different environmental conditions that might occur in rain, groundwater, or waste disposal sites; their exact chemical composition and pH are shown in Table 1. All leaching solutions were base on deionized (DI) water. Over the whole 1.5 years of the experiments, the pH and the oxidation/reduction-potential E_H remained almost constant. Data for E_H, following DIN38404-6, stemmed from measurements with a platinum electrode against a silver/silver chloride reference (Ag/AgCl). The concentration of potassium chloride $c_{KCl} = 3$ mol/L was $T = 25\,^{\circ}$C; we converted the data to a potential against a standard hydrogen electrode [17].

Throughout the leaching experiments, starting after 0.5 days, we periodically took 15 mL samples from the leaching solutions in the bottles and analyzed them for the leached out elements. After taking the probe, we pored in again fresh solution of 15 mL to keep the 1000 mL volume. All data were corrected for the amount of elements that were taken out from the solution due to sampling.

Table 1. Composition of leaching solutions with pH-values of 3, 7, and 11 used in the experiments and the measured reduction potential E_{H} ; the same conditions as in [10]. (Copyright (2017) The Japan Society of Applied Physics, reproduced with permission).

pH	E_{H} (V)	Chemical Composition
3	0.62	15.4 g/L $C_6H_8O_7$, 2.8 g/L Na_2HPO_4, DI water
7	0.56	3.7 g/L KH_2PO_4, 5 g/L Na_2HPO_4, DI water
11	0.33	0.04 g/L NaOH, DI water

2.2. Heavy Metal Analysis and Determination of Initial Metal Content in Module Pieces

We characterized the samples that were taken from the leaching solutions with inductively coupled plasma mass spectrometry (ICP-MS) and give the data for the leached elements according to ISO 17294-2 [18]. This method is only able to measure dissolved substances; it cannot detect precipitations in the solution. Therefore, the elements in the precipitates were not counted as leached.

Here, we always give the amount of leached out elements as a percentage with respect to the total amount of elements that were in the original module pieces. Therefore, we had to measure the total mass of those elements in the module pieces before the experiment. For that purpose, similar module pieces as those for the experiments were milled to a powder. Then, the powder was digested by adding acid and oxidizing agents and, finally, using microwave irradiation. After that, the digested samples underwent the ICP-MS analysis, similar to our earlier experiment [10]. For each PV technology, and for all the elements analyzed, Table 2 shows their mass M_{total} that was contained in the original reference module pieces.

Table 2. Elemental mass M_{total} in the 5×5 cm^2 module pieces for crystalline silicon (c-Si), amorphous silicon (a-Si), cadmium telluride (CdTe), and copper indium gallium diselenide (CIGS). The data represent mean values and the standard deviation from three measurements.

Element	c-Si (mg)	a-Si (mg)	CdTe (mg)	CIGS (mg)
Zn		0.9 ± 0.4		16.1 ± 3.1
Cd			13.9 ± 0.9	0.2 ± 0.002
Te			15.6 ± 1.1	
In				14.1 ± 4.3
Ga				0.7 ± 0.1
Se				6.7 ± 1.3
Al	167 ± 40	196 ± 27	289 ± 63	280 ± 190
Mo			12.7 ± 1.7	5.0 ± 0.2
Cu	254 ± 15	130 ± 14	80 ± 11	146 ± 5.7
Ni		1.0 ± 0.1		
Pb	16.7 ± 0.8		2.4 ± 0.3	

2.3. Mass Balancing at the End of the Leaching Experiments

During the leaching experiments, the total mass:

$$M_{total} = M_{diss} + M_{MP} + M_{FR} \quad (1)$$

of a particular element is the sum of the following masses: the amount M_{diss} dissolved in the solution, the remaining mass M_{MP} within the module pieces, and the mass M_{FR} that precipitated in the bottles of the solution. Clearly, at the end of the leaching experiment, the total mass, determined by Equation (1) should equal the masses in Table 1. We measured the mass M_{FR} in the following way: First, the module pieces were removed from the bottles, and then, the solution was filtered using vacuum filtration with a cellulose nitrate membrane filter with a pore size of 0.45 µm. The mass M_{MP} was measured in the same way as the total mass of the elements in one module piece, as described previously. To measure the mass of the filter residue M_{FR}, we digested the filter residue together with the filter by applying a microwave enhanced oxidative digestion. Again, ICP-MS measured these samples, and the measurement of the cellulose nitrate membrane filter itself (blank value) ran in parallel. Subtracting the blank values for the filter, we calculated the amount of each element in the filter residue.

3. Results

3.1. Delamination of Module Pieces

One focus during long-term leaching in water-based solutions lies in the occurrence of delamination. In order to simulate field conditions, in a first series of experiments, we did not use any accelerating leaching parameters for the module pieces for analyzing the delamination (Figure 1a). Delamination, in this study, is defined as a separation between all kinds of module layers, not only between the encapsulation layer, often ethylene vinyl acetate (EVA) foil, and the glass. The delamination was determined by visual examination.

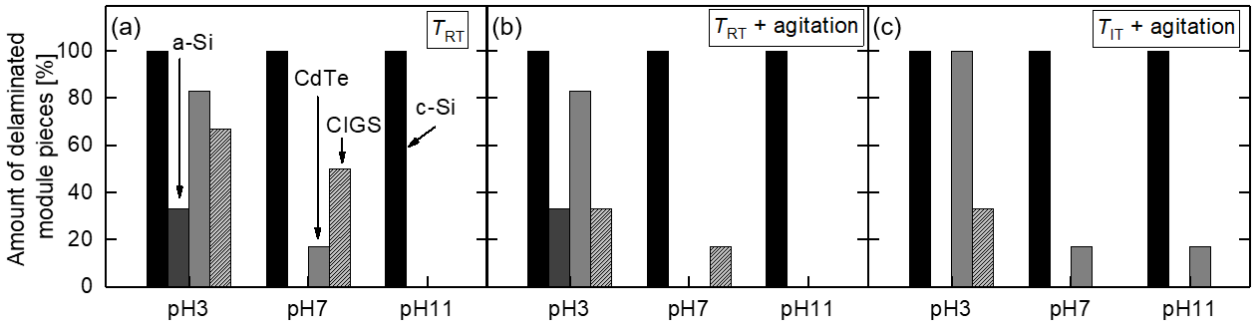

Figure 1. Amount of delaminated module pieces from crystalline silicon (c-Si), amorphous silicon (a-Si), cadmium telluride (CdTe), and copper indium gallium diselenide (CIGS) depending on the pH value of the water-based solution after 1.5 years for the three different experimental conditions: (**a**) $T_{RT} = 25\,^{\circ}\mathrm{C}$, no agitation, (**b**) $T_{RT} = 25\,^{\circ}\mathrm{C}$, with agitation, and (**c**) $T_{IT} = 40\,^{\circ}\mathrm{C}$, with agitation.

After 1.5 years of leaching, we observed delamination in all kinds of PV module pieces: c-Si, a-Si, CdTe, and CIGS. The probability of delamination depends on the pH value of the solutions and the experimental conditions. In the case of c-Si module pieces, we always observed 100% delamination, independent of the pH-value, temperature, and agitation: in all aqueous solutions and for all module pieces, delamination occurred. However, in this case, delamination occurred via the EVA layer, and the type differed from the delamination type of thin film module pieces (via thin layers), as discussed later. Delamination of a-Si module pieces only happened in aqueous solutions with pH 3, and only 30% of the module pieces were affected. The agitation (Figure 1b) and also the temperature (Figure 1c) had no accelerating effect on the delamination. In fact, during the leaching experiments with $T_{IT} = 40\,^{\circ}\mathrm{C}$ plus agitation, no delamination of a-Si module pieces was found. The highest amount of delamination in the case of CdTe module pieces occurred in acidic water-based solutions. For this type of module, the increased temperature weakly affected the delamination, as shown in Figure 1c. At room temperature, no delaminated CdTe module pieces were observed in the solutions with pH 11, whereas in neutral solutions, only 17% of the module pieces showed delamination. The pH dependence held also for the CIGS module pieces. In pH 3 solutions, the highest amount of delamination occurred with 67% of the module pieces. In pH 7 solutions, the amount of delaminated module pieces was still 50%. In alkaline solutions with pH 11, no delamination was observed with agitation or with increased temperature.

We classified all these delaminations into three different types: (i) Total separation: Here, the front side is clearly separated from the rear side. This delamination occurs in case of CdTe and a-Si module pieces. Figure 2a shows a scheme of this delamination type. (ii) Fractional separation: Here, only parts of the rear or front side are separated. The major part of the module compound is still intact. This type of delamination takes place for CIGS module pieces and for c-Si module pieces when leached in solutions with pH 11. The scheme is shown in Figure 2b. (iii) Blistering: Figure 2c shows this third type of delamination. Blistering occurs between either the front glass and the EVA foil, or between the EVA foil and the solar cell, but there is no complete separation. This type only occurs in c-Si module pieces.

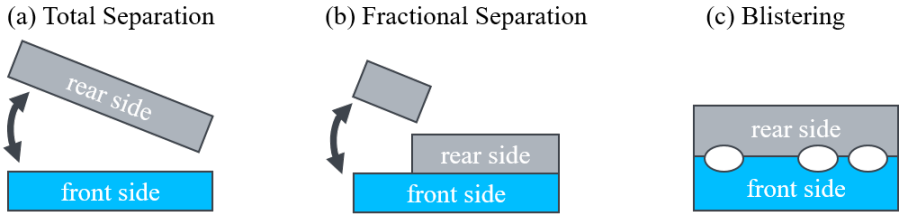

Figure 2. Different types of delamination during the leaching process: (**a**) Total separation (observed for CdTe and a-Si module pieces). The front side is completely separated from the rear side. (**b**) Fractional separation (observed for CIGS and c-Si module pieces). Only small parts of the rear side are separated; the major part of the module structure is still intact. (**c**) Blistering (only observed for c-Si module pieces). Bubble formation emerges locally on the front side of c-Si module pieces, either between glass and EVA or between EVA and solar cell depending on the pH. In this case, no separation occurs between the front and the rear side.

Total separation: Figure 3a–d shows photographs of the front and the rear side of a 5 × 5 cm^2 CdTe module piece before and after 1.5 years of leaching. Before leaching the CdTe module piece, the integrated series connection of the cells is visible (see the horizontal lines) on the front side (Figure 3a) and also on the rear side (Figure 3b). On the rear side, one sees also the solder ribbon. Only the rear side glass of the module piece shows cracks caused by the water jet cutting. The breakage pattern of this glass indicates that heat-strengthened glass is used as the rear side glass. Figure 3c,d shows the front and the rear side of a CdTe module piece after the leaching process of 1.5 years in solutions with pH 3. Apart from a few parts, the module material disappeared completely. The solder ribbon is still attached to the rear side glass by an insulating tape. After this long-term leaching, the front and the rear side glasses are no longer connected to each other, but totally separated. For a-Si module pieces, the same type of delamination is observed.

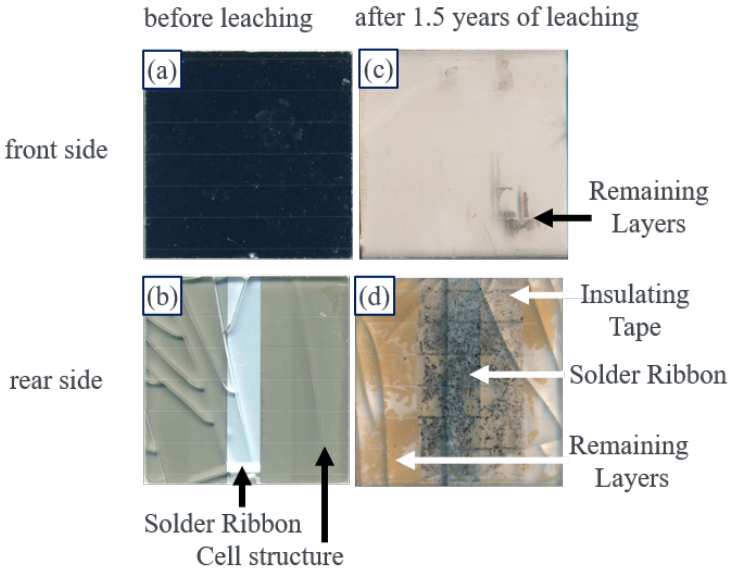

Figure 3. Photographs of (**a**) the front and (**b**) the rear side of a 5 × 5 cm^2 CdTe module piece before leaching. On the rear side, the solder ribbon and the interconnection of cells are visible. (**c**) Front side of the module piece after leaching over 1.5 years in solutions with pH 3. Apart from a few visible remaining parts, the module material disappeared. (**d**) Rear side of the module piece after the leaching. The solder ribbon with the insulating tape is visible and also some parts of remaining layers. After 1.5 years of leaching, the front and the rear side glasses are no longer attached to each other; total separation occurs.

Fractional separation: Figure 4a–d shows photographs of the front and the rear side of a 5 × 5 cm^2 CIGS module piece before and after 1.5 years of leaching: parts of the rear side are separated. Both glasses, the front and the rear side glass, show cracks due to the water jet cutting. Figure 4c shows a photograph of the front side after 1.5 years of leaching in solutions with pH 3. From the front side, a few transparent spots around the edges are visible. From a more detailed look at the back side of the module piece (Figure 4d), it becomes clear that at the transparent spots, parts of the rear side glass are missing, together with the back contact and the active module layers. Therefore, only the transparent front glass remains.

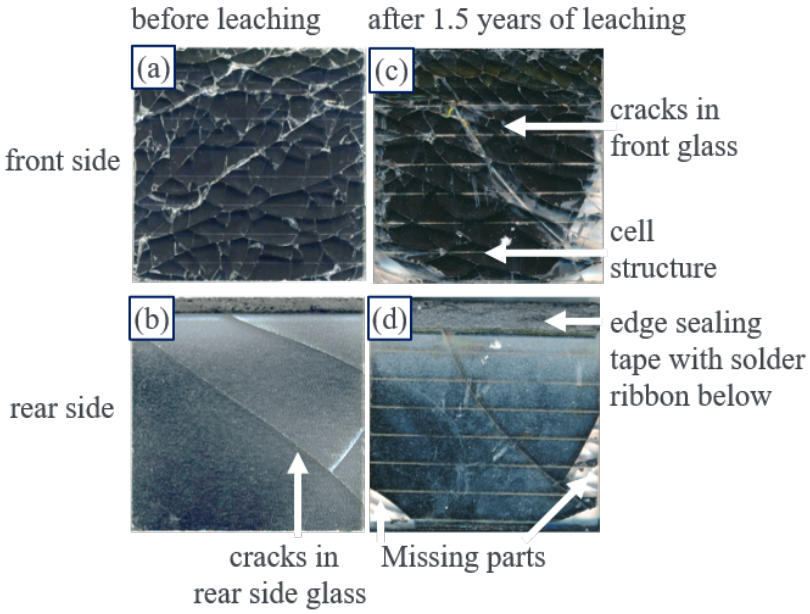

Figure 4. Photographs of (**a**) the front and (**b**) the rear side of a 5 × 5 cm^2 CIGS module piece before leaching. On the rear side, the edge sealing tape with the solder ribbon below is visible. In the front glass, as well as in the rear side glass, cracks are recognizable; they stem from the water jet cutting. (**c**) Front side after leaching for 1.5 years in pH 3 solution. (**d**) Rear side after leaching. Parts of the rear glass are missing, together with the back contact and the active layers. Only the transparent front glass remains.

Blistering: Figure 5a shows a photograph of a c-Si module piece of 5 × 5 cm^2 in size after 1.5 years of leaching in pH 3 solution. In this case, local bubble formation takes place between the solar cell and the EVA foil, especially around the solder ribbon, but no total separation is observed. In solutions with pH 11, delamination between the EVA foil and the front glass appears across extended areas (Figure 5b). A few parts of the glass are separated, and the exposed EVA foil with the solar cell below remains. Due to delamination, the textured structure of the front glass becomes visible. The breakage pattern of the glass matches the pattern known for tempered glass. The rear side of the c-Si module pieces (white backsheet) shows no changes caused by leaching. Only for this PV technology, the occurrence of delamination, i.e., blistering, does not depend on the pH value of the leaching solution. Module pieces leached in pH 7 solutions also show blistering. Blistering takes place at both locations: between the solar cell and the EVA foil, as well as between the EVA foil and the front glass.

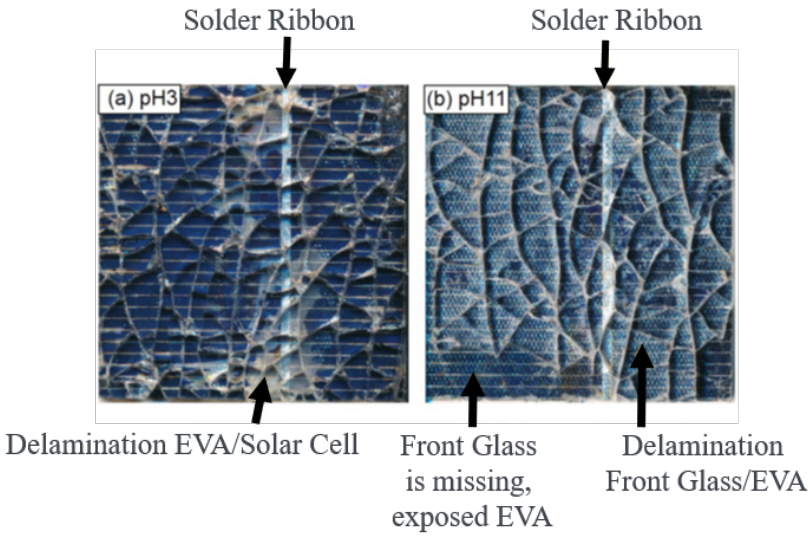

Figure 5. Photographs of c-Si module pieces with 5 × 5 cm^2 after 1.5 years of leaching in solutions with (**a**) pH 3 and (**b**) pH 11. In solutions with pH 3, a local bubble formation occurs between the solar cell and the EVA foil, preferably around the solder ribbon. In solutions with pH 11, a delamination between the EVA foil and the front glass appears across extended areas. A few parts of the glass are separated, and the exposed EVA foil with the solar cell below remains.

3.2. Leaching Results

The previous figures, as well as our previous experiments on milled module pieces [8] give the proof for severe leaching for all module technologies. In the following, we present detailed results on the elements that were leached out from module pieces of 5 × 5 cm^2 in size. In a first publication [10], we presented preliminary leaching data for Cd, Te, and Pb only and until Day 360, i.e., about one year. In contrast, here, we extend our study to 1.5 years and include many more other elements. This gives us the chance to identify possible weak spots and the leaching paths in the modules. In detail, we measure the amount of the following elements in our water-based solutions of Table 1 with different pH-values: Zn, Te, In, Ga, Se, Al, Mo, Cu, Cd, and Pb. The non-toxic element Si, which is contained in the modules' cells from crystalline, as well as from amorphous silicon, is not measured, simply because the module glass itself also contains high amounts of Si. Our measurement conducted by ICP-MS cannot distinguish between Si from the cells and from the glass of the modules.

3.2.1. CdTe Module Pieces

Figure 6a shows the common structure of a CdTe module including the front glass and front contact (usually tin oxide (SnO_2)), the buffer layer cadmium sulfide (CdS), the photoactive layer CdTe, the Mo back contact, the encapsulant EVA, and finally, the rear side glass. The typical thickness of each layer is also given [19–21]. CdTe modules are mostly fabricated in a superstrate configuration: the production process starts with the front glass, on which the transparent front contact SnO_2 is deposited. We used commercial CdTe-modules for the preparation of the module pieces and measured the amount of eluted elements with the above discussed ICP-MS method. Therefore, we are not able to distinguish between the Cd from the CdS buffer layer and the Cd from the photoactive CdTe film.

Figure 6b–d shows the time-dependent leaching of the elements Cd, Te, and Mo in water-based solutions with pH 3, pH 7, and pH 11; see also [10] for the leaching results of Cd and Te until Day 360. These results stemmed from experiments at $T_{RT} = 25\,^{\circ}C$ without agitation. In all solutions, the amount of leached elements increases with time, but with different leaching rates for different pHs of the solutions. At the early beginning of leaching, Mo from the back contact leaches out with the highest amount, followed by Cd.

Tellurium leaches the least. Thus, already from this observation, it becomes clear that the Mo layer is a weak spot in the case of the CdTe module. After approximately 300 days of leaching, the concentration of Te increases dramatically and approaches the eluted amount of Cd and Mo. Around this time of leaching, delaminations are observed. After 1.5 years, the concentrations of eluted Cd and Mo related to the total amount in the module piece in acidic solutions (pH 3) reach $c_{Cd} \approx 92\%$ and $c_{Mo} \approx 88\%$. The amount of eluted Te is $c_{Te} \approx 54\%$.

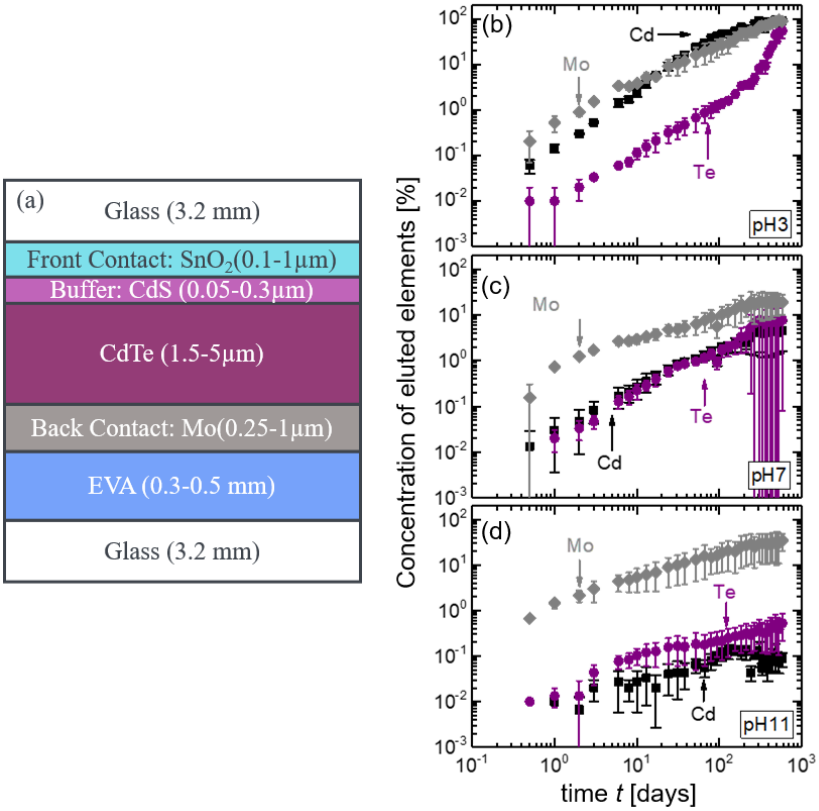

Figure 6. (**a**) Schematic structure of a typical CdTe module (not drawn to scale) and (**b**) time-dependent leaching results of the elements Cd, Te, and Mo from CdTe module pieces in acidic aqueous solutions with pH 3 and (**c**) in solutions with pH 7 and (**d**) pH 11.

Figure 6c shows the leaching in water-based solutions with pH 7. Here, the concentrations of eluted Cd, Mo, and Te, finally, after 1.5 years, reach $c_{Cd} \approx 4,5\%$, $c_{Mo} \approx 19\%$, and $c_{Te} \approx 7.8\%$, respectively. In this case, the leaching of Cd and Te shows the same time-dependent leaching behavior. The large standard deviations for Te appearing after approximately 300 days of leaching are due to the delamination of one module piece out of three experimental runs. Clearly, after delamination of this particular module piece, substantially higher amounts are leached out, because the leaching solution is able to directly attack the CdTe layers from the surface. Therefore, we observe substantially higher amounts of eluted Te and slightly higher amounts of Cd for this one out of the three experimental runs. The leaching of Mo is highest from the beginning to the end and comparable to the leaching amounts of Cd and Te.

Figure 6d presents the leaching data for pH 11. Here, at the end of the experiment, the amount of eluted Mo is still high with $c_{Mo} \approx 34\%$. The measured concentration of Te is below 1% after 1.5 years, and the amount of leached Cd is the lowest. In solutions with pH 11, the time-dependent leaching rates of Cd and Te are much lower compared to the leaching rates in solutions with pH 7 and pH 3. For all conditions, the leaching rate of Mo is always higher than the one of Cd and Te. This indicates again that, in the case of CdTe modules, the Mo back contact is a weak spot.

The leaching results in Figure 6b–d clearly demonstrate an enormous difference between the leaching concentrations after one day and after the 1.5 years. For example, the Cd-elution in pH 3 at the end of the experiment reaches almost 100%, whereas it is only about 1 % after one day. For pH 3 and pH 7, the eluted concentrations increase approximately linearly with time: a one order of magnitude increase (on the log-scale) of the time leads to a one order of magnitude higher concentration (on the log scale) of the concentration. For pH 11, the data approach a square root dependence with time: it needs a two orders of magnitude increase on the time scale for a one order of magnitude increase on the concentration scale.

Figure 7 shows the ratio $R_{Cd:Te}$ of dissolved Cd to dissolved Te from leaching CdTe module pieces in solutions with pH 3, pH 7, and pH 11. For leaching solutions with pH 3, the value of $R_{Cd:Te}$ is not constant over the leaching time. At the beginning of leaching, $R_{Cd:Te}$ is highest with 35:1, but with time, it approaches $R_{Cd:Te} \approx 1$. For neutral solutions with pH 7, $R_{Cd:Te} \approx 1$ and is almost constant over time. The same behavior applies for leaching in alkaline solutions, but with $R_{Cd:Te} \approx 0.1$. This means that more Te is dissolved in the solutions.

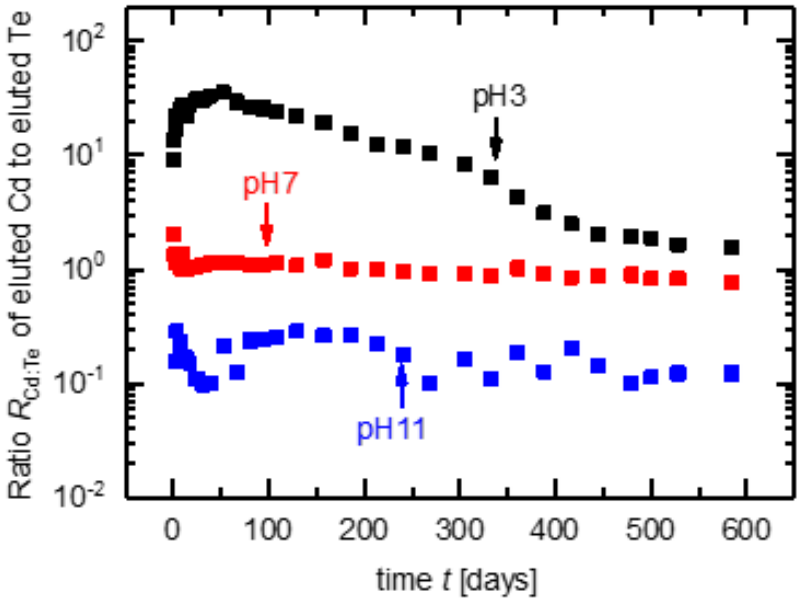

Figure 7. Ratio $R_{Cd:Te}$ of dissolved Cd to dissolved Te from leaching CdTe module pieces in solutions with pH 3, pH 7, and pH 11.

3.2.2. CIGS Module Pieces

Figure 8a shows a schematic cross-section through a CIGS module, composed of the front glass with EVA, the front contact (usually consisting of aluminum-doped zinc oxide, ZnO:Al), a buffer layer of CdS, the absorber layer Cu(In, Ga)Se_2, and a thin interfacial layer of $MoSe_2$ between the substrate glass and the CIGS. The $MoSe_2$ is formed by a reaction between the Mo and the Se atmosphere during the deposition of the Cu, In, and Ga [22]. CIGS modules are built in a substrate configuration. The fabrication starts with the deposition (sputtering or evaporation) of Mo on the rear glass. Then, the CIGS is deposited, mostly by co-sputtering or thermal evaporation of the constituent elements, Cu, In, and Ga in a Se atmosphere.

Figure 8b shows the leaching data for Zn, Cd, Mo, Cu, Ga, and In in pH 3 solutions. At the beginning of leaching, Zn from the front contact shows the highest amount with $c_{Zn} \approx 1\%$ already after one day; finally, we observe $c_{Zn} \approx 62\%$ after 1.5 years. Furthermore, already after one day, certain amounts of Mo from the back contact and In from the absorber layer are measurable in the solutions. Other elements, like Cd, Cu, and Ga, are detected later on. The leaching rates of each element differ in absolute values, but show a similar

time dependence. The leaching of the Mo from the CIGS module pieces differs from the data for Mo from CdTe module pieces (see Figure 6b). The Mo from CdTe module pieces seems to be more soluble, in particular for acidic solutions. The difference probably results from the formation of $MoSe_2$ at the back side of the CIGS films.

Figure 8c shows the leaching of Zn, Cd, Mo, Cu, Ga, and Se in pH 7 solutions. Indium is not detected in the solution with pH 7. The leaching of Zn for this pH is lower than that for pH 3, and so is the concentration after 1.5 years. In solutions with pH 11, we only find Mo, Ga, and Se with low concentrations in the solutions, as shown in Figure 8d. The leached Mo is lowest for pH 11 compared to the data from solutions with pH 3 and pH 7. In the case of CIGS module pieces, comparable to CdTe, the Mo back contact is a weak spot, but also the front contact Zn and the buffer layer Cd.

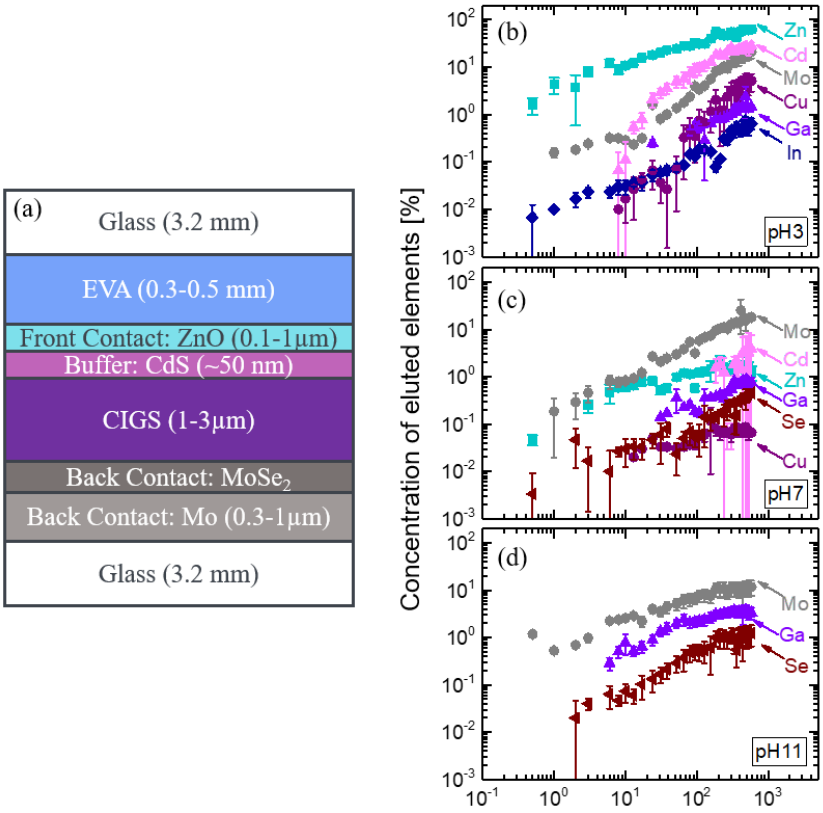

Figure 8. (**a**) Schematic structure of a typical CIGS module (not drawn to scale) and (**b**) time-dependent leaching results of the elements Zn, Cd, Mo, Cu, Ga, and In from CIGS module pieces in acidic aqueous solutions with pH 3 and (**c**) in solutions with pH 7 and (**d**) pH 11. In leaching solutions with pH 11, the concentrations of the elements Cd, Zn, Cu, and In are below the detection limit.

3.2.3. c-Si Module Pieces

Figure 9a shows a schematic cross-section through a classic c-Si module, consisting of a front glass with EVA, a silver front contact grid with contact fingers and busbars, and the silicon solar cell with a screen printed aluminum back contact and screen printed Ag contact pads (not drawn in the scheme). In contrast to thin film modules, instead of a rear glass, most c-Si modules have a backsheet and a second EVA sheet at the rear side. Figure 9b,c shows the leaching data for Al and Pb for pH 3 and pH 11 (see also [10] for the leaching results of Pb until Day 360). In the case of pH 7, the concentrations of Al and Pb are below the detection limit, which is 500 µg/L for Al and 20 µg/L for Pb. The eluted Pb stems either from the solder ribbon, which is not shown in the schematic cross-section, or from the screen printed metallization. For pH 3, the amount of leached Pb remains constant and below 0.1% until Day 241. After this time, the concentration increases dramatically up to $c_{Pb} \approx 3.7\%$ after 1.5 years. The concentration of Al reaches $c_{Al} \approx 27\%$ after 1.5 years in

the acidic solution. In contrast, for the alkaline solution with pH 11, the concentrations of Al and Pb are significantly lower, as shown in Figure 9c. In both cases, the leaching rates of Al are orders of magnitude higher than the ones for Pb. Thus, in the case of c-Si module pieces, the Al contact, which is screen printed and fired into the back side, makes up the weak spot and opens the path for leaching.

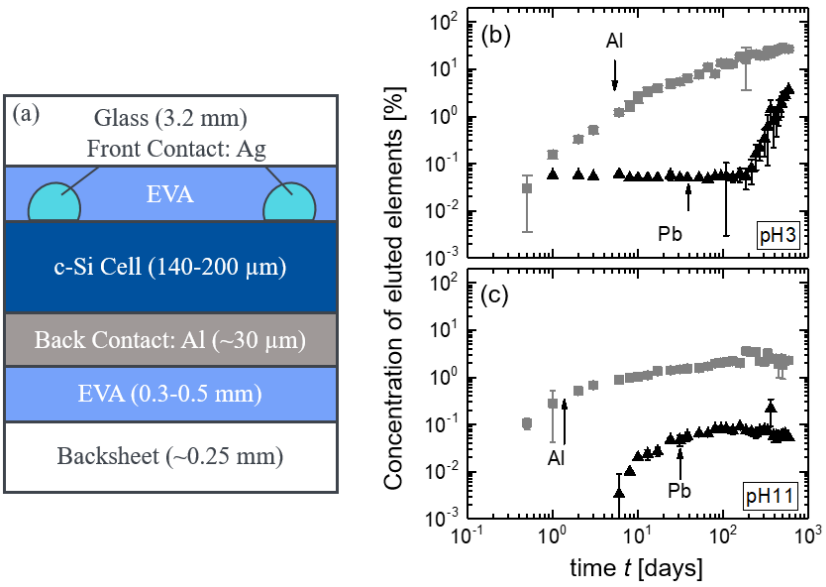

Figure 9. (**a**) Schematic structure of a typical c-Si module (not drawn to scale) and (**b**) time-dependent leaching results of Al and Pb from c-Si module pieces in acidic aqueous solutions with pH 3 and (**c**) in solutions with pH 11. In leaching solutions with pH 7, the concentrations of Al and Pb are below the detection limit.

3.2.4. a-Si Module Pieces

The common structure of an a-Si module is shown in Figure 10a. Amorphous silicon modules typically consist of a front glass with the front contact layer (SnO_2 is mostly used), the photoactive p-i-n layer from a-Si, followed by an intermediate layer consisting of ZnO and Ag, the back contact with a combination of Ni and Cu, and the encapsulant with the rear glass [23]. Similar to the production of CdTe modules, a-Si modules are built in a superstrate configuration, starting with the deposition of the front contact directly on the front glass. Figure 10b,c shows the concentrations of eluted Zn, Cu, and Ni in the solutions with pH 3 and pH 7. Unfortunately, we do not have any data about Ni before Day 388 of leaching. In leaching solutions with pH 11, the concentrations of Zn, Cu, and Ni are below the detection limits. For the other pH-values, we are able to present data: Zn, which stems from the intermediate layer, shows strong leaching with concentrations up to $c_{Zn} \approx 90\%$ after 1.5 years of leaching in the acidic pH 3 solution. The concentration of eluted Ni lies in the same range, whereas the concentration of Cu is $c_{Cu} \approx 7.5\%$. In aqueous solutions with pH 7, the elements Zn, Ni, and Cu leach only in minor amounts. The elements Zn, Cu, and Ni are leached out linearly with time, but with different rates depending on the element itself, as well as on the pH of the solution. In all cases, the leaching of the Zn is highest, and therefore, we identify the ZnO layer as a weak spot in a-Si module pieces.

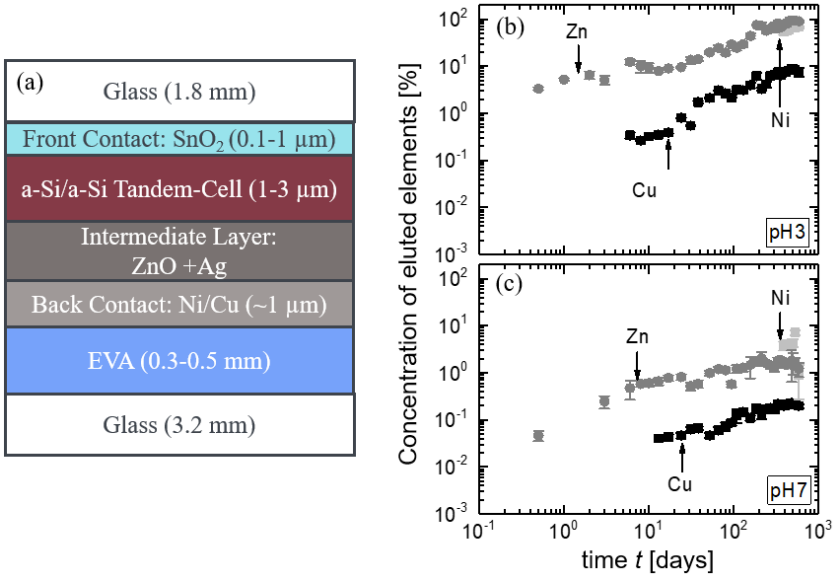

Figure 10. (**a**) Schematic structure of a typical a-Si module (not drawn to scale) and (**b**) time-dependent leaching results of Zn, Cu, and Ni from a-Si module pieces in acidic aqueous solutions with pH 3 and (**c**) in solutions with pH 7. In leaching solutions with pH 11, the concentrations of Zn, Cu, and Ni are not measurable according to the detection limit.

3.3. Accelerating Leaching Parameters for Cd from CdTe Module Pieces

All of the experiments considered so far were performed without any acceleration, for example, by elevated temperatures or stirring/agitation. Figure 11a,b compares the data for Cd, leached out from CdTe module pieces, for the three different pH-values and with/without agitation. Apart from the tests at $T_{RT} = 25\,^{\circ}\mathrm{C}$, we also used additional agitation and solutions at an elevated temperature $T_{IT} = 40\,^{\circ}\mathrm{C}$. All test series ran in parallel. Figure 11a shows the results after $t = 1$ day and Figure 11b after $t = 416$ days. The comparison of the two figures again underlines the dramatic difference in the leaching results after one day and after more than a year. Therefore, standard leaching experiments, which are only carried out over one day, are more or less meaningless, when one aims at judging the toxicity of CdTe modules. Furthermore, after just one day (see Figure 11a), additional agitation and/or elevated temperatures only slightly increase the amount of eluted Cd, even if for pH 3 solutions. In contrast, in particular for pH 7, increasing the temperature from $T_{RT} = 25\,^{\circ}\mathrm{C}$ to $T_{RI} = 40\,^{\circ}\mathrm{C}$ results in five times stronger leaching. Leaching in pH 11 solution triples the leaching of Cd for the same temperature increase. In contrast, in the case of agitation, we are not able to detect any Cd in the alkaline solutions after one day. In the case of pH 3, for all experimental conditions, after $t = 416$ days, the amount of eluted Cd in acidic solutions reaches almost 100%. In the case of the neutral pH 7 solutions, the final data all lie in the same range of $2\% < c_{Cd} < 4\%$. After 416 days, the eluted Cd reaches saturated values. Therefore, as shown in Figure 11b, there is almost no or only minor differences between the data with and without additional accelerating parameters.

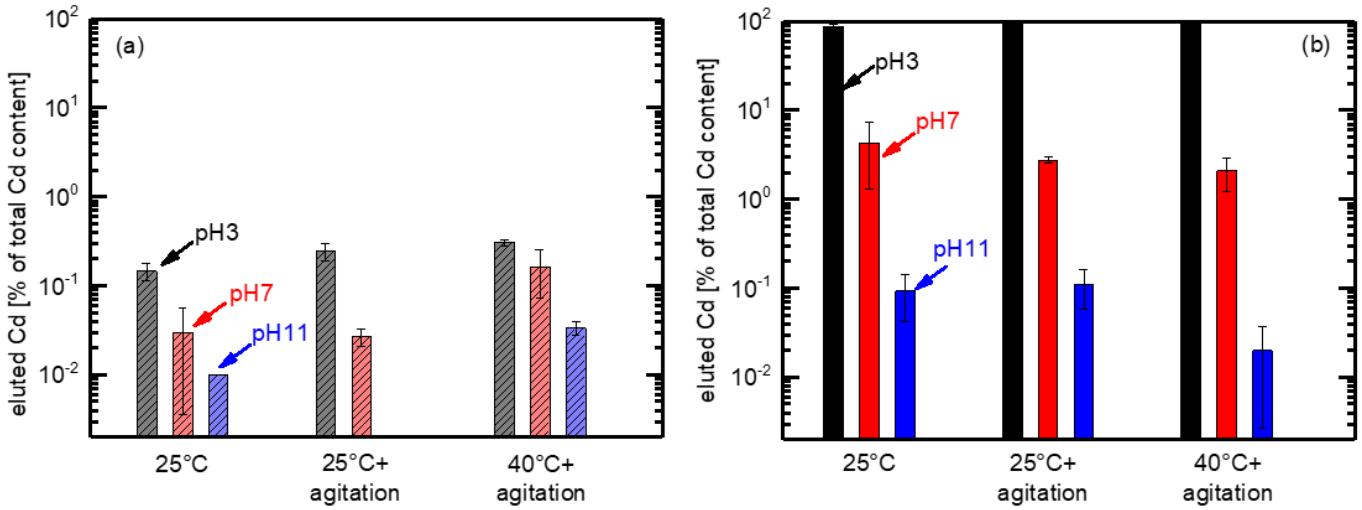

Figure 11. Dramatic difference between the leaching data after one day and more than a year of Cd out of CdTe module pieces. (**a**) Amount of eluted Cd from CdTe module pieces after $t = 1$ day in solutions of pH 3, 7, and 11 and different leaching conditions: with/without agitation and increased temperature $T_{IT} = 40\,^{\circ}$C plus agitation. For all conditions, after one day, the Cd concentration ranges below 1%. (**b**) Amount of eluted Cd from CdTe module pieces after $t = 416$ days. For pH 3, almost 100% of the Cd is leached out. For pH 7, still several percent are leached out. This finding raises the question of the meaningfulness of judging the toxicity of CdTe containing modules with tests that are carried out for one day only.

3.4. Analysis of Time Dependence

To get a better understanding of how the different leaching conditions affect the time-dependent leaching, we fit the measured concentration $C(t)$ at the time t to an exponential model according to:

$$C(t) = C_{max}(1 - e^{-\frac{t}{\tau}}), \tag{2}$$

where C_{max} is the maximum, final concentration dissolved in the solution and τ is the leaching time constant. The leaching time constant represents the time for the concentration to reach 63% of its final value as a measure of leaching velocity. For times $t \ll \tau$, the Taylor expansion of Equation (2) yields a linear behavior according to:

$$C(t) = C_{max}\frac{t}{\tau}. \tag{3}$$

Indeed, in almost all of our experiments, if not disturbed by delamination effects, we see the linear time dependence predicted by Equation (3) and the saturation predicted by Equation (2). Equation (3) is the direct consequence of the number of atoms (Cd)that are leached per unit time, being directly proportional to the number of atoms that are still available for etching. Such an approach always leads to an exponential function such as Equation (2). However, not only delamination (which is expected to accelerate the leaching), but also other effects such as the formation of surface layers (see our work [24]), diffusion limitations, and/or the formation of precipitates could result in deviations from a behavior following Equations (2) and (3). For a diffusion limited leaching on a thin layer, one would observe a square root dependence, as discussed in [24]. This might be the case for some of the data here, in particular for pH 11.

Most of experimental data, in particular for pH 3 and pH 7, show an excellent agreement with the linear behavior, predicted by Equation (3) for time $t \ll \tau$, as well as for the saturation behavior, Equation (2). As an example, Figure 12a–c shows the time-dependent leaching of Cd from CdTe module pieces in solutions with pH 3 for the three different leaching conditions. The data are excellently fit with coefficients of determination $R^2 \geq 0.96$. Figure 12d–f shows the leaching data of Cd in solutions with pH 7. The dotted lines

represent the calculated fit according to Equation (2). The dashed lines show the calculated maximum Cd concentration C_{max} in the solutions; the time constants τ are also given. Modifications to the leaching conditions lead to accelerated leaching with a shorter time constant τ: For example, increasing the temperature to $T_{IT} = 40\,^{\circ}$C, as shown in Figure 12c, leads to a time constant that is only a third of the value at $T_{RT} = 25\,^{\circ}$C. In contrast to the time constant, the C_{max}-value is almost independent of the leaching conditions in pH 3 solution; it holds $C_{max} \approx 100\%$. Figure 12d shows the leaching data for pH 7 at $T_{RT} = 25\,^{\circ}$C without agitation; we find $\tau = 210$ days. After this time $t = \tau$, a value of 63% of the maximum Cd concentration is reached, which is estimated to be $C_{max} = 4.8\%$. Modified experiments slightly decrease the maximum concentration, which we explain by the large standard deviations at the end of leaching, caused by the delamination of module pieces. Additional agitation decreases the time constant to $\tau = 80$ days (Figure 12e); increased temperature yields $\tau = 20$ days (Figure 12f), i.e., four-times faster leaching.

The excellent fits of our leaching data for pH 3 and pH 7 to Equations (2) and (3) show also that in this case, the leaching is not limited by any diffusion processes, which might take place inside or on the surface of the CdTe layers (this statement holds also for the experiments on all other cell technologies). This behavior is in contrast to our results on the leaching of milled module pieces, which were reported in a separate publication [24]. There, the model for the small spherical CdTe particles, with sizes below one millimeter, predicts a power law, with leaching data following a dependence on time t according to $t^{0.43}$. Indeed, in [24] we observed this behavior for the small particles also experimentally. Due to the different size and geometry of the samples, the leaching from the flat plates of module pieces as presented here, at least for pH 3 and pH 7, follows a different time dependence, which, for short times compared to the leaching time constant, is $t^{1.0}$, as, for example, shown in Figure 6b,c.

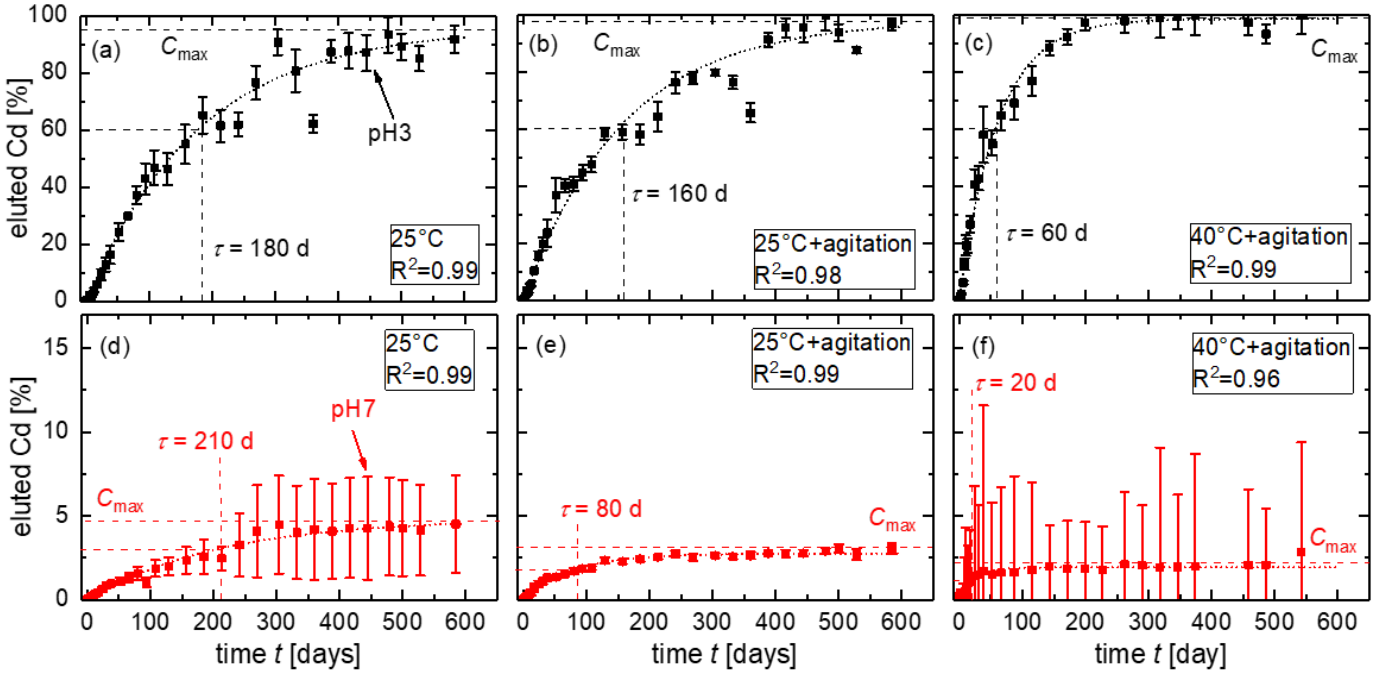

Figure 12. Leaching of Cd from CdTe module pieces in solutions with pH 3 at (**a**) $T_{RT} = 25\,^{\circ}$C, (**b**) at $T_{RT} = 25\,^{\circ}$C with agitation, and (**c**) at $T_{IT} = 40\,^{\circ}$C with agitation. Eluted Cd in solutions with pH 7 at (**d**) $T_{RT} = 25\,^{\circ}$C, (**e**) at $T_{RT} = 25\,^{\circ}$C with agitation, and (**f**) at $T_{IT} = 40\,^{\circ}$C with agitation. The dotted lines represent the calculated fit according to Equation (2) with high coefficients of determination R^2. The dashed lines show the calculated maximum concentration C_{max} in the solutions.

Figure 13a shows the leaching time constant τ for pH 3 and pH 7: A higher temperature results in faster leaching. In our study, $T_{IT} = 40\,^{\circ}$C is used, which is a common temperature PV modules reach when exposed to sunlight; on hot summer days, the temperatures are

even higher. In solutions with pH 7, the change in the leaching time constant due to varied conditions is even stronger. In contrast to a different τ, Figure 13b shows that the maximum concentration C_{max} of eluted Cd remains nearly constant and independent of modifications to the leaching conditions. However, the value C_{max} highly depends on the pH of the leaching solution: it holds $C_{max} \approx 100\%$ for pH 3 and $C_{max} \leq 4.8\%$ for pH 7. The lower C_{max} for pH 7 is explained by the formation of cadmium hydroxide in neutral solutions. This compound is not soluble and therefore not detected by our measurement method ICP-MS.

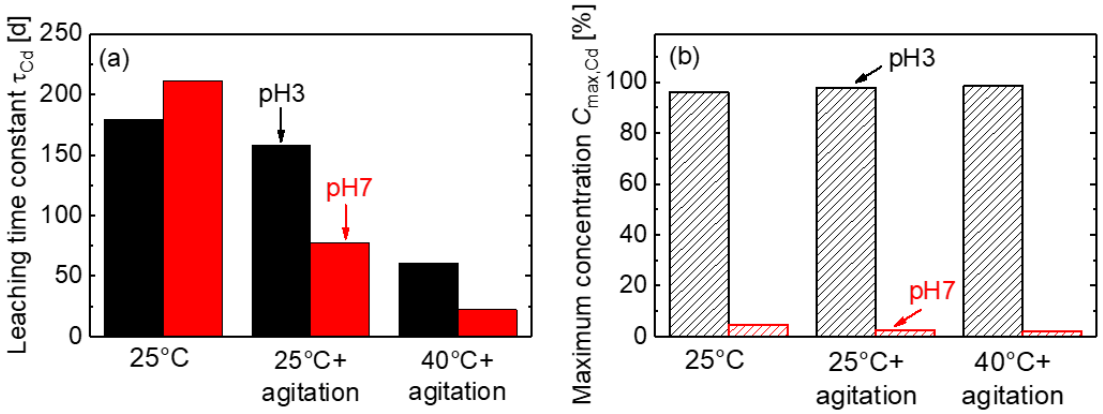

Figure 13. Calculated fit parameters for the leaching of Cd from CdTe module pieces under different conditions. (**a**) Leaching time constant τ_{Cd} for solutions with pH 3 and pH 7. (**b**) Maximum concentration C_{max} for the same conditions as in (**a**).

3.5. Mass Balance for CdTe Module Pieces

Figure 14 shows the distribution of the mass fractions for the elements Cd, Te, and Mo from CdTe module pieces leached for 700 days at $T_{RT} = 25\,^{\circ}\mathrm{C}$ without agitation: the dissolved amount in the solution M_{diss}, the remaining mass in the module piece M_{MP} after the leaching process, and the mass of the filter residue M_{FR} with particles bigger than 0.45 mm. There are strong differences between the leaching behavior for pH 3 and pH 11:

pH 3: Almost all Cd, Te, and Mo from the module pieces is found in the mass M_{diss} of dissolved elements. In particular, for Cd, almost nothing remains in the module piece (mass M_{MP}) or is found in the mass M_{FR} of precipitates.

pH 11: Almost all Cd and Te still remain in the module pieces and are represented by the mass M_{MP}. Only in the case of Mo, a part of the Mo is measured in the solution as M_{diss}.

Mass loss for Te and Mo: The sum of the masses in the solution, filter, and module pieces measured after the leaching should reach 100% of the value before the leaching. However, for Te and Mo, the sum of the measured values after leaching is below 100%. The relatively small amount of missing mass is termed M_{Rest} in Figure 14. We explain the difference by the milling process for the determination of the remaining mass M_{MP} in the module piece. For a few samples, the milling process did not completely crush the encapsulation. The Mo back contact has a strong adhesion to the encapsulant. Therefore, it seems possible that not all Mo material was digested. There might also be a material loss during the filtration process, either when drying the filter afterwards, or due to particles remaining in the HDPE bottles despite carefully repeated rinsing.

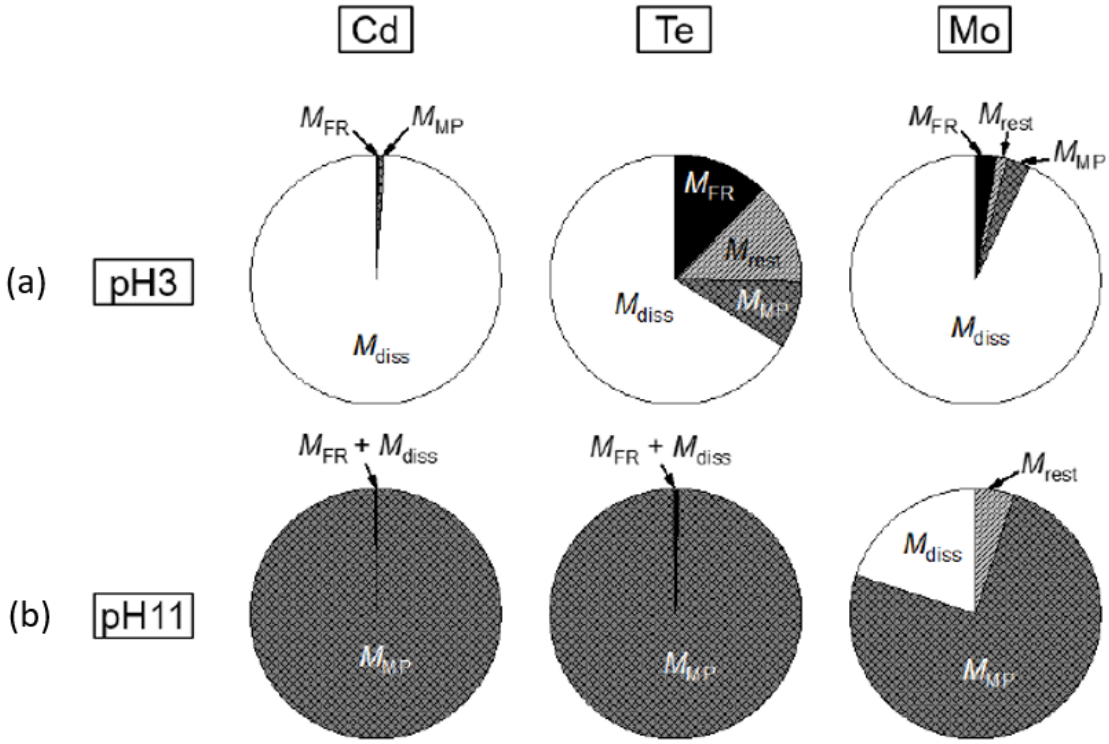

Figure 14. Mass balance of the CdTe module piece after 700 days in leaching solutions with (**a**) pH 3 and (**b**) pH 11 at $T_{RT} = 25\,^{\circ}\mathrm{C}$ without agitation. In solutions with pH 3, the largest fraction of Cd, Te, and Mo is dissolved and found as M_{diss}; only a small fraction M_{MP} remains in the module pieces. No Cd-particles (mass M_{FR}) are measured within the filter residue, whereas for Te and Mo, a small part is found in the residue. In solutions with pH 11, the major part of the elements Cd and Te remains in the module piece and is not leached out. Molybdenum is also measured in the solution.

4. Discussion

The combination of leaching experiments and the observation of delamination yields the following major insight: In the case of thin film modules (CdTe, CIGS, and a-Si), the delamination is the consequence of the high solubility of one or more thin layers of the modules' cells. They form a path for the attack of the water-based solutions. In contrast, in the case of modules containing cells from crystalline silicon, the cell's Al back contact is highly soluble, but not responsible for delamination. Instead, blistering occurs: delamination of c-Si modules is not visible on the back side, but on the front side, either between the front glass and EVA or between the EVA and the Si cell, depending on the pH of the leaching solution. Delamination between the front EVA and solar cell preferentially occurs around the solder ribbon on the front side of the cell and is therefore correlated with the leaching of Pb out of the solder ribbon. The backsheet on the rear side of the c-Si module piece shows no changes after the leaching. Unfortunately, the backsheet is not transparent; therefore, we do not have information about the condition of the solder ribbon on the back side and how the leaching of the Al back contact affects the leaching of the solder ribbon on the back. In solutions with pH 3, a local delamination takes place between the solar cell and the EVA foil, whereas in pH 11 solutions, the delamination occurs between front glass and EVA. In pH 7 solutions, we observe both kinds of delamination. The solution probably attacks the coupling agent. Therefore, in this case, we assume adhesion problems to be the main reason for blistering.

In the case of CdTe module pieces, the photoactive CdTe, as well as the Mo back contact are highly soluble in acidic, aqueous solutions with pH 3. The severe leaching correlates with the frequent total separation, i.e., delamination of the module pieces. For this type of module and under acidic conditions, frequently, the front side is clearly separated from the rear. As a consequence, this delamination enhances the leaching, especially of Te, which is

observed in all leaching solutions, independent of pH. For short times, leaching for Cd, Te, and Mo increases linearly with time, but at different rates; the rates depend on the pH. The ratio $R_{Cd:Te}$ of eluted Cd to eluted Te Cd:Te also depends on the pH. This behavior is in accordance with the Pourbaix (potential-pH) diagram for CdTe in aqueous solutions showing the possible species of Cd and Te depending on the pH and the redox potential E_H [9]. In solutions with pH 3, the Te species have a lower solubility compared to the Cd species, which are present as Cd^{2+} ions. The solubility of predominant species of Cd and Te for pH 7 is the same, which explains the ratio $R_{Cd:Te} = 1$. In solutions with pH 11, probably, Te species form with a solubility that exceeds that of Cd. This assumption explains the estimated $R_{Cd:Te} \approx 0.1$. It is notable that only in solutions with pH 3, the ratio $R_{Cd:Te}$ is strongly time dependent, whereas it is almost constant for solutions with pH 7 and pH 11.

Increasing the temperature results in accelerated leaching of Cd from CdTe module pieces. The same behavior was earlier reported by Collins and Anctil [25] for the leaching of Cd from CIGS modules and Pb from c-Si modules, by increasing the leaching temperature to $T = 50\,^{\circ}C$. All of our leaching data for Cd are well described by Equation (2) and the C_{max}-value for Cd, which decreases with increasing pH. This finding is in accordance with the data reported by Ramos-Ruiz [5] on leaching of Cd and Te out of CdTe modules in solutions with different pH values under simulated landfill conditions. This pH-dependent leaching is understood on the basis of known leaching patterns, not only for Cd, but for all measured elements in this study.

In contrast to CdTe modules, with total delamination, for CIGS module pieces, fractional separation occurs in solutions with pH 3, as well as with pH 7: only parts of the rear side are separated. Our leaching experiments point out all CIGS module layers to be more or less soluble in aqueous solutions. The highest solubility is found for Zn from the front contact in pH 3 solutions, and at this location, we observe the fractional separation. With the Zn eluted, there is no longer a stable bond between the front glass/EVA and the rear side consisting of the photoactive layers (CdS, CIGS) and the back contact on top of the rear glass.

The leaching concentrations of Cd out of CIGS module pieces are lower than from CdTe module pieces. This lower leaching of Cd indicates that CdS in the CIGS cells is more stable against the solutions than CdTe. The Mo back contact of CIGS module pieces also seems to be more stable than the Mo back contact of CdTe module pieces. Between these two module types, the amounts of leached Mo differ especially in solutions with pH 3 and pH 11: in these solutions, Mo from CIGS shows lower leaching than Mo from CdTe module pieces. This difference probably arises from the formation of the $MoSe_2$ layer during the deposition of the CIGS layer in module fabrication. Theelen et al. [26] proposed that $MoSe_2$ prevents the formation of molybdenum oxide, MoO_x, which is the main reason for the degradation of Mo when it comes in contact with water or moisture. Modules from CdTe do not contain a protecting $MoSe_2$ layer. Therefore, during leaching, MoO_x is probably formed. The formation of MoO_x results in a large volume expansion [26]. This could explain the observed delaminations for CdTe module pieces.

Amorphous silicon module pieces show also highly time-dependent leaching, in particular the front layer of ZnO in combination with the Ni/Cu back contact. After 1.5 years of leaching, the elements Zn and Ni reach almost 100% in solutions with pH 3. The time-dependent leaching behavior of Zn from a-Si module pieces is similar to the leaching behavior of Zn from CIGS module pieces in both solutions of pH 3 and pH 7. The leaching rates are also comparable. Therefore, in the case of a-Si modules, ZnO is a weak spot. This finding is in line with the experiments of Pern et al. [27]: These authors studied the stability of various transparent conducting oxides (TCO), including ZnO. In their experiments, ZnO showed the highest degradation rates (of all studied TCOs) when it comes in contact with moisture.

5. Conclusions

Our leaching experiments on PV modules pieces from CdTe, CIGS, c-Si, and a-Si in water-based solutions with pH 3, pH 7, and pH 11 simulate different environmental conditions. Due to the wide span of pH-values, it seems also possible to predict from our experiments the behavior for other pH-values. During the leaching over 1.5 years, we observe different types of delamination. In the case of thin film modules (CdTe, CIGS, a-Si), the thin film layers themselves or the contact materials (e.g., Mo, ZnO) are the weak spots. Finally, their leaching leads to delamination. In contrast, in the case of modules with c-Si, the Al back contact shows the strongest leaching. However, this leaching is not responsible for the delamination. Instead, problems with the EVA causes blistering, which leads to the delamination of the module pieces with c-Si.

The time-dependent leaching is well described by an exponential saturation behavior with a leaching time constant, at least for low pH-values. The leaching time constant differs from element-to-element and changes under agitation and/or a temperature increase. For times small compared to this time constant, the amount of leached out elements increases linearly with time. It is therefore understandable that, roughly speaking, the concentrations of many leached out elements after 500 days are also more than two orders of magnitude higher than after one day. However, we observe also ratios of the concentrations after one 500 days and after one day that are higher or lower than two orders of magnitude: Higher values are obtained, when delamination occurs during leaching. Lower values are obtained when, for example, the ratio of eluted to precipitating elements changes during the experiment.

In the case of Cd leaching from CdTe module pieces, increased temperature leads to substantially accelerated leaching. In contrast, the maximal concentration of leached Cd only depends on the pH of the solution. A mass balance method shows that Cd, which is not measured in the solutions as dissolved, remains in the module pieces themselves and is not, as expected, leached out and then precipitated in the solutions.

In any case and under all experimental conditions, it is possible to either leach out all or a substantial amount of most elements from the module pieces. Clearly, in the case of our module pieces, leaching starts from the unprotected edges of the pieces of 5×5 cm^2 in size, cut out from large area modules. During the manufacturing of commercial modules, they are provided with an edge sealing, which should prevent any leaching under normal operating conditions of the (undamaged) modules. However, if the edge sealing of the modules is not carefully done, or if it is damaged, or even worse, if the (front) module glass is broken, leaching is unavoidable. Rain water with pH values always below pH 7 will suffice to leach out the (toxic) elements. Even worse, if modules are cracked, crushed, or even milled and end up in landfills, the module constituents will also be leached out. Therefore, if toxic materials are not completely avoided in photovoltaic modules, it is of utmost importance to (i) replace damaged modules as fast as possible and to (ii) recollect and recycle them completely. In all other cases, in view of the huge amount of installed PV modules, most of them still containing Pb (mostly in the solder of the cell connectors) and/or Cd, they may impose a severe danger to the environment.

Compared to other, earlier studies, our experiments were carried out over more than a year. As one of the key results, we found huge differences between the amount of elements found in the solutions after one day and more than a year. In our opinion, tests for just one day are inappropriate to judge module technologies, in particular if conclusions and political decisions on the toxicity and environmental issues of photovoltaic module technologies are based on such short-term measurements.

Author Contributions: Conceptualization amd project administration, R.Z.-G. and J.H.W.; methodology, R.Z.-G., M.K., J.N.; validation and investigation, J.N., R.Z.-G., M.K., C.F.; analysis, writing, editing, and reviewing J.N., R.Z.-G., M.K., J.H.W. All authors have read and agreed to the published version of the manuscript.

Funding: This research was funded by German Federal Ministry of Economics and Technology (BMWi), Project Number 0325718.

Acknowledgments: The authors thank Lara Busch for sample preparation and measurements.

Conflicts of Interest: The authors declare no conflict of interest. The funders had no role in the design of the study; in the collection, analyses, or interpretation of data; in the writing of the manuscript; nor in the decision to publish the results.

References

1. Phillips, S.; Warmuth, W. *Photovoltaics Report*; Fraunhofer ISE: Freiburg, Germany, 2020.
2. Wade, A.; Heath, G.; Weckend, S.; Wambach, K.; Sinha, P.; Jia, Z.; Komoto, K.; Sander, K. *IRENA and IEA PVPS-End-of-Life Management: Solar Photovoltaic Panels*; National Renewable Energy Lab.: Golden, CO, USA, 2016.
3. Directive 2011/65/EU of the European Parliament and of the Council of 8 June 2011 on the Restriction of the Use of Certain Hazardous Substances in Electrical and Electronic Equipment Text with EEA Relevance. Available online: http://data.europa.eu/eli/dir/2011/65/oj (accessed on 29 January 2021).
4. ITRPV. International Technology Roadmap for Photovoltaic (ITRPV) 2019 Results. Available online: https://itrpv.vdma.org/en/ (accessed on 12 October 2020).
5. Ramos-Ruiz, A.; Wilkening, J.; Field, J.; Sierra-Alvarez, R. Leaching of Cadmium and Tellurium From Cadmium Telluride (CdTe) Thin-Film Solar Panels Under Simulated Landfill Conditions. *J. Hazard. Mater.* **2017**, *336*, 57. [CrossRef] [PubMed]
6. Zimmermann, Y.S.; Schäffer, A.; Corvini, P.F.X.; Lenz, M. Thin-film photovoltaic cells: Long-term metal (loid) leaching at their end-of-life. *Environ. Sci. Technol.* **2013**, *47*, 13151. [CrossRef] [PubMed]
7. Tammaro, M.; Salluzzi, A.; Rimauro, J.; Schiavo, S.; Manz, S. Experimental investigation to evaluate the potential environmental hazards of photovoltaic panels. *J. Hazard. Mater.* **2016**, *306*, 395. [CrossRef] [PubMed]
8. Zapf-Gottwick, R.; Koch, M.; Fischer, K.; Schwerdt, F.; Hamann, L.; Kranert, M.; Metzger, J.; Werner, J.H. Leaching Hazardous Substances out of Photovoltaic Modules. *Int. J. Adv. Appl. Phys. Res.* **2015**, *2*, 7. [CrossRef]
9. Zeng, C.; Ramos-Ruiz, A.; Field, J.A.; Sierra-Alvarez, R. Cadmium telluride (CdTe) and cadmium selenide (CdSe) leaching behavior and surface chemistry in response to pH and O_2. *J. Environ. Manag.* **2015**, *154*, 78. [CrossRef] [PubMed]
10. Nover, J.; Zapf-Gottwick, R.; Feifel, C.; Koch, M.; Metzger, J.; Werner, J.H. Long-term leaching of photovoltaic modules. *Jpn. J. Appl. Phys.* **2017**, *56*, 08MD02. [CrossRef]
11. Nain, P.; Kumar, A. Initial metal contents and leaching rate constants of metals leached from end-of-life solar photovoltaic waste: An integrative literature review and analysis. *Renew. Sustain. Energy Rev.* **2020**, *119*, 109592. [CrossRef]
12. EN 12457-4:2002. *Characterization of Waste-Leaching; Compliance Test for Leaching of Granular Waste Materials and Sludges–Part 4: One Stage Batch Test at a Liquid to Solid Ratio of 10 L/kg for Materials with Particle Size below 10 mm (without or with Limited Size Reduction)*; Swedish Institute for Standards: Stockholm, Sweden, 2002.
13. United States Environmental Protection Agency. *Test Methods for Evaluating Solid Waste: Physical/Chemical Methods*; SW-846; United States Environmental Protection Agency: Washington, DC, USA, 1992.
14. CCR, California Code of Regulations. *Waste Extraction Test (WET) Procedures*; Title 22. Division 4.5, Chapter 11, Article 5, Appendix II. 1991.
15. Japanese Standards Association. *JIS K 0102:2016-Testing Methods for Industrial Wastewater*; Japanese Standards Association: Tokyo, Japan, 2016.
16. Nover, J.; Huber, S.; Zapf-Gottwick, R.; Werner, J.H.; Feifel, C.; Koch, M.; Metzger, J. *Schadstofffreisetzung aus Photovoltaik-Modulen Abschlussbericht: Laufzeit: 01.09.2014-31.08.2017*; Universität Stuttgart, Institut für Photovoltaik: Stuttgart, Germany, 2018.:1020510552. [CrossRef]
17. DIN 38404-6:1984-05. *German Standard Methods for the Examination of Water, Waste Water and Sludge; Physical and Physico-Chemical Parameters (Group C); Determination of the Oxidation Reduction (Redox) Potential (C 6)*; Swedish Institute for Standards: Stockholm, Sweden, 1984.
18. ISO 17294-2:2003. *Water Quality-Application of Inductively Coupled Plasma Mass Spectrometry (ICP-MS)-Part 2: Determination of 62 Elements*; ISO: Geneva, Switzerland, 2003.
19. Deb, S.K. Recent Advances and Future Opportunities for Thin-Film Solar Cells. In *Thin-Film Solar Cells: Next Generation Photovoltaics and Its Applications*; Hamakawa, Y., Ed.; Springer: Berlin/Heidelberg, Germany, 2004; p. 27.
20. Chopra, K.L.; Paulson, P.D.; Dutta, V. Thin-film solar cells: An overview. *Prog. Photovolt Res. Appl.* **2004**, *12*, 69. [CrossRef]
21. Fritsche, J.; Klein, A.; Jaegermann, W. Thin Film Solar Cells: Materials Science at Interfaces. *Adv. Eng. Mater.* **2005**, *7*, 914. [CrossRef]
22. Theelen, M.; Daume, F. Stability of Cu(In,Ga)Se2 solar cells: A literature review. *Sol. Energy* **2016**, *133*, 586. [CrossRef]
23. Gabriel, O.; Kirner, S.; Leendertz, C.; Gerhardt, M.; Heidelberg, A.; Bloeß, H.; Schlatmann, R.; Rech, B. Large area PECVD of a-Si:H/a-Si:H tandem solar cells. *Phys. Status Solidi C* **2011**, *8*, 2982. [CrossRef]
24. Zapf-Gottwick, R.; Zorn, M.; Nover, J.; Koch, M.; Feifel, C.; Werner, J.H. Solubility of Cadmium Telluride in Aqueous Solutions. *Energies* **2021**, *14*, 398. [CrossRef]

25. Collins, M.K.; Anctil, A. Implications for current regulatory waste toxicity characterisation methods from analysing metal and metalloid leaching from photovoltaic modules. *Int. J. Sustain. Energy* **2017**, *36*, 531. [CrossRef]
26. Theelen, M.; Polman, K.; Tomassini, M.; Barreau, N.; Steijvers, H.; Van Berkum, J.; Vroon, Z.; Zeman, M. Influence of deposition pressure and selenisation on damp heat degradation of the Cu(In,Ga)Se_2 back contact molybdenum. *Surf. Coat. Technol.* **2014**, *252*, 157. [CrossRef]
27. Pern, F.J.; Noufi, R.; Li, X.; DeHart, C.; To, B. Damp-heat induced degradation of transparent conducting oxides for thin-film solar cells. In Proceedings of the 33rd IEEE Photovoltaic Specialists Conference, San Diego, CA, USA, 11–16 May 2008.